

# 俯冲带镁铁质堆晶岩的母岩浆恢复:方法与实例\*

郭锋<sup>1,2</sup>

GUO Feng<sup>1,2</sup>

1. 中国科学院广州地球化学研究所,同位素国家重点实验室,广州 510640

2. 中国科学院深地科学卓越创新中心,广州 510640

1. State Key Laboratory of Isotope Geochemistry, Guangzhou Institute of Geochemistry, Chinese Academy of Sciences, Guangzhou 510640, China

2. Excellent Center of Deep Earth Sciences, Chinese Academy of Sciences, Guangzhou 510640, China

2022-07-29 收稿, 2022-09-21 改回.

**Guo F. 2022. Estimation of parent magma compositions of mafic cumulate at subduction zones: Methods and examples. *Acta Petrologica Sinica*, 38(12):3647–3658, doi:10.18654/1000-0569/2022.12.05**

**Abstract** The architecture recovery of paleo-subduction zone/orogenic belt is fundamental to reconstruct the paleo-plate tectonics of the Earth. Yet it remains difficult to rebuild the paleo-subduction zone/orogenic belt because most arc magmatic rocks, especially the basaltic lavas, are lacking, in response to orogeny and subsequent crustal deformation, uplifting and unroofing, with only residual ultramafic-mafic cumulates that may represent the lower arc crust. Strictly, mafic cumulate is an aggregate of rock-forming and accessory minerals and trapped melts, and their whole-rock compositions can no longer represent the parental arc basalts. This means that it is problematic to use the mafic cumulate geochemistry to track the tectonic evolution of subduction zones. Based on the previous equilibrium distribution method, the author have recently developed two methods for parent magma recalculation of mafic cumulates respectively approaching by clinopyroxene and hornblende. During the calculation, the author further consider the role of accessory minerals such as apatite, ilmenite, titanite and zircon to eliminate the compositional anomaly in primitive mantle-normalized incompatible element (e.g., P and Ti) spidergrams, except for usually positive Sr-Eu anomalies indicative of plagioclase accumulation. These methods have been widely applied in the compositional estimation of parent magmas for the mafic cumulates in paleo-subduction/orogenic belts across the eastern China, including NE China, South China, the Central Asian Orogenic Belt, and the Yunkai Region. By comparing the calculated results with the measured whole-rock compositions, the trace elemental ratios like Th/La, Ba/La and Ba/Nb remains nearly constant during the backstripping procedure, indicating that these ratios are useful tools to track the enrichment processes operated beneath the mantle wedge of the paleo-subduction zones. In contrast, the calculated Th/Yb ratio is obviously higher than the measured value, so the measured whole-rock Th/Yb ratio cannot be employed to evaluate the role of subducted sediments at subduction zones.

**Key words** Geochemical composition; Equilibrium distribution; Parent magma; Mafic cumulate; Subduction zone

**摘要** 古老俯冲带/造山带结构的恢复是重建古板块构造的基石。然而,古俯冲带/造山带由于受到造山作用和随后强烈的构造改造、隆升与剥蚀作用,绝大多数弧岩岩浆尤其是玄武岩较为缺乏,通常仅保留了代表弧下地壳的超镁铁质-镁铁质堆晶岩。从严格意义上来说,镁铁质堆晶岩是造岩矿物、副矿物与粒间熔体的集合体,其全岩成分不能代表弧岩岩浆本身,因此运用其地球化学来讨论俯冲带演化存在诸多不确定性和多解性。在前人提出的平衡配分方法基础上,作者近年来建立了基于单斜辉石和角闪石的俯冲带镁铁质堆晶岩的母岩浆恢复方法,并根据样品在原始地幔标准化微量元素蛛网图中的异常变化情况,通过增减相关的副矿物成分予以校正。该方法广泛应用于中国东北、华南、中亚造山带和云开地区等古俯冲带/造山带镁铁质堆晶岩的母岩浆成分恢复。通过对比计算结果与全岩的实测成分,发现两种方法获得的 Th/La、Ba/La 和 Ba/Nb 比值差别不大,反映这些微量元素比值可以用于示踪古俯冲带地幔楔的改造过程。然而计算获得的 Th/Yb 比值则明显比镁铁质堆晶岩的全岩实测值偏高,因此该比值不适合用来示踪俯冲带中沉积物的贡献。

\* 本文受国家自然科学基金项目(42073032,41525006,42021002)资助。

第一作者简介:郭锋,男,1971年生,研究员,主要从事岩石学与大地构造学研究,E-mail: fengguo@gig.ac.cn, guofengt@263.net

**关键词** 地球化学组成;平衡配分法;母岩浆;镁铁质堆晶岩;俯冲带

**中图法分类号** P588.112; P588.125

俯冲带是汇聚板块边界发生相互作用的地带,也是地震、构造、岩浆及成矿作用较为发育的区域,表现为一个板块向相邻板块之下的下降潜伏过程(Tatsumi and Eggins, 1995; Stern, 2002)。俯冲带主要由俯冲的大洋岩石圈、地幔楔、上覆板片以及沟-弧体系等多个部分组成。在俯冲带有大量的弧岩浆作用发育,开展弧火成岩尤其是镁铁质火成岩的研究,可以很好地认知俯冲带地幔楔的改造过程和演化历史(McCulloch and Gamble, 1991)。

关于俯冲带岩浆作用的研究,前人已经开展了大量的工作,总结起来,取得的进展包括以下几个共识:(1)俯冲带岩浆具有富水的特征,其初始岩浆的水含量在4%左右(Plank *et al.*, 2013),与俯冲板片脱水过程密切相关(Grove *et al.*, 2006; Zack and John, 2007; Shaw *et al.*, 2008);(2)岩石主要为拉斑-钙碱性系列,并在微量元素组成上显示出亏损高场强元素和富集大离子亲石元素的特征,在同位素组成上相对洋中脊玄武岩更为富集(Davies and Stevenson, 1992; Tatsumi and Eggins, 1995; Macdonald *et al.*, 2000);(3)俯冲带地幔楔交代介质来自俯冲板片,包括洋壳和上覆沉积物的熔体和流体(von Huene and Scholl, 1991; Nichols *et al.*, 1994; Stolz *et al.*, 1996),并根据沉积物的差异,可以分为洋内弧和大陆弧(Plank and Langmuir, 1998; Tollstrup and Gill, 2005; Zhao *et al.*, 2019)。

相对于现今的俯冲带发育有较为完整的岩浆作用记录,古俯冲带距今时间较为久远,因此容易受到地壳隆升剥蚀或构造活动的改造,弧火山岩难以保存下来,通常被保留下来的是镁铁质堆晶岩或者岩体的根部。从严格意义来说,镁铁质-超镁铁质堆晶岩是由主要造岩矿物、副矿物和粒间熔体的集合体(图1),其全岩组成不能代表与矿物之间平衡的母岩浆成分(Bédard, 1994),因此利用传统的地球化学方法进

行成因研究和古俯冲带再循环组分的识别存在诸多不确定性。如何恢复与这些镁铁质堆晶岩之间平衡的母岩浆成分开展古俯冲带/造山带岩浆成因研究的难题之一。

Bédard (1994, 2001) 基于质量平衡方程和单斜辉石分配系数,率先提出了运用矿物-熔体之间的平衡配分关系(equilibrium distribution method, EDM)来计算与堆晶矿物组合平衡的熔体成分。作者团队以及其他单位研究人员在开展东北吉黑地区早侏罗世古太平洋俯冲带基性岩浆成因的研究中发现了多处零星出露的镁铁质侵入杂岩(图1a, Yu *et al.*, 2012; Guo *et al.*, 2015),采纳该方法来恢复区域辉长岩的母岩浆成分。在后续的研究中发现古俯冲带中的一部分镁铁质侵入杂岩的主要暗色矿物为角闪石(图1b, Guo *et al.*, 2016; Zhang *et al.*, 2019),辉石和橄榄石少见,反映岩浆极为富水的特点(Ridolfi and Renzulli, 2012)。为此我们在前人的基础上拓展出基于角闪石分配系数的母岩浆成分计算方法。由于在镁铁质堆晶岩中除了常见的斜长石、暗色矿物如橄榄石、辉石和角闪石堆晶作用外,也存在一些副矿物如榍石、磷灰石、锆石、磁铁矿和铬铁矿等的影响,从而导致这类堆晶岩在原始地幔标准化不相容元素蛛网图上除了表现出常见的Sr-Eu正异常外,还会出现Ti、Zr-Hf、Th-U以及P的异常。通过特定副矿物的增减可以消除这些异常,从而得到更真实的堆晶岩母岩浆成分。这两种计算方法已经陆续被国内外学者用于恢复相关镁铁质堆晶岩的母岩浆成分。由于以前的相关文章都发表在英文杂志上,受众范围相对较窄;为了方便广大国内地质工作者参考,本文将简明扼要地进行方法原理和研究实例的介绍,并附录Excel表(见期刊官网附件1)来演示如何计算,为其后续应用提供方便。最后我们通过计算结果与实测值的对比来讨论运用镁铁质堆晶岩地球化学来示踪俯冲带演化的适用性。

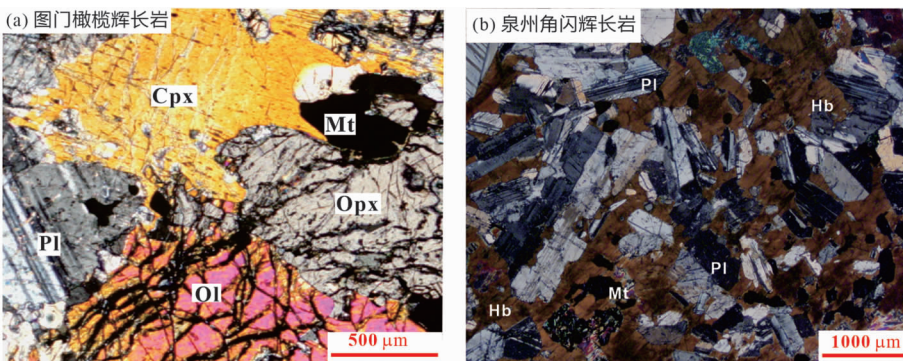


图1 中国东部古俯冲带典型镁铁质侵入岩(具堆晶结构)的正交偏光显微照片

(a) 橄榄辉长岩(延边地区侏罗纪图门岩体, Guo *et al.*, 2015); (b) 白垩纪角闪辉长岩(福建泉州, Zhang *et al.*, 2019)

Fig. 1 Microphotos of typical mafic intrusions (accumulation texture) from the paleo-subduction zones in eastern China

(a) an olivine gabbro from the Jurassic Tumen intrusive complex in NE China (Guo *et al.*, 2015); (b) a hornblende gabbro from the Cretaceous Quanzhou intrusion in SE China (Zhang *et al.*, 2019)

## 1 平衡配分方法

基于质量平衡方程,假设岩浆体系为封闭系统,熔体发生固结形成了矿物堆晶+粒间熔体(trapped melt, 简称为TM)的集合体(Bédard, 1994)。进行平衡配分法需满足以下前提:(1)矿物之间达到平衡;(2)在接近岩浆固相线的温度下,粒间熔体迅速被包裹在原位结晶矿物格架的孔隙中;(3)岩浆固结后没有经历后期的流体/熔体交代或渗滤作用。此时粒间熔体成分代表了平衡的“固相线”熔体成分。为了方便表达,本文将计算获得的粒间熔体成分视作代表与矿物集合体平衡的母岩浆成分。这种方法成功用于加拿大拉布拉多元古代斜长岩和镁铁质堆晶岩以及太古代 Albitibi 绿岩带中镁铁质堆晶岩的成分恢复(Bédard, 2001; Bédard *et al.*, 2009)。

假设某辉长岩/橄长岩/苏长岩的全岩成分为不同矿物与粒间熔体的加权总和,那么其全岩成分可以表达为:

$$C_i^{\text{全岩}} = \varphi^{\text{Cpx}} C_i^{\text{Cpx}} + \varphi^{\text{Opx}} C_i^{\text{Opx}} + \varphi^{\text{Ol}} C_i^{\text{Ol}} + \varphi^{\text{Pl}} C_i^{\text{Pl}} + \varphi^{\text{副矿物}} C_i^{\text{副矿物}} + \varphi^{\text{TM}} C_i^{\text{TM}} \quad (1)$$

$C_i$  为某元素在全岩、单矿物和粒间熔体的含量,  $\varphi$  代表了单

矿物和粒间熔体的质量百分数。在辉长岩中主要造岩矿物为橄榄石(Ol)、斜方辉石(Opx)、单斜辉石(Cpx)和斜长石(Pl),部分岩石含有角闪石(Hb)。副矿物包括铁钛氧化物如磁铁矿(Mt)、钛铁矿(Il)、铬铁矿(Chr)、磷灰石(Ap)、榍石(Ttn)、锆石(Zr)/斜锆石(Bed)等。各种造岩矿物和副矿物的质量百分数可以通过标准矿物 CIPW 计算或实际岩相学观察获得。基于矿物/熔体之间平衡与分配系数( $D_i$ )的关系,可以获得单斜辉石某元素的含量:

$$\begin{aligned} C_i^{\text{Cpx}} &= C_i^{\text{Pl}} (C_{\text{Cpx}/\text{熔体}} D_i / C_{\text{Pl}/\text{熔体}} D_i) = C_i^{\text{Opx}} (C_{\text{Cpx}/\text{熔体}} D_i / C_{\text{Opx}/\text{熔体}} D_i) \\ &= C_i^{\text{Ol}} (C_{\text{Cpx}/\text{熔体}} D_i / C_{\text{Ol}/\text{熔体}} D_i) = C_i^{\text{副矿物}} (C_{\text{Cpx}/\text{熔体}} D_i / C_{\text{副矿物}/\text{熔体}} D_i) \end{aligned} \quad (2)$$

把等式(2)并入到等式(1)进行简单变换,可以获得单斜辉石某元素的含量:

$$\begin{aligned} C_i^{\text{Cpx}} &= C_i^{\text{全岩}} / (\varphi^{\text{Cpx}} + \varphi^{\text{Opx}} \times C_{\text{Opx}/\text{熔体}} D_i / C_{\text{Cpx}/\text{熔体}} D_i + \\ &\varphi^{\text{Ol}} \times C_{\text{Ol}/\text{熔体}} D_i / C_{\text{Cpx}/\text{熔体}} D_i + \varphi^{\text{Pl}} \times C_{\text{Pl}/\text{熔体}} D_i / C_{\text{Cpx}/\text{熔体}} D_i + \\ &\varphi^{\text{副矿物}} \times C_{\text{副矿物}/\text{熔体}} D_i / C_{\text{Cpx}/\text{熔体}} D_i + \varphi^{\text{TM}} \times C_{\text{Cpx}/\text{熔体}} D_i) \end{aligned} \quad (3)$$

在等式(3)中,只有 $\varphi^{\text{TM}}$ 为未知变量,因此我们可以假定不同的 $\varphi^{\text{TM}}$ ,就可以获得单斜辉石的某元素含量,最后就能通过公式: $C_i^{\text{熔体}} = C_i^{\text{Cpx}} / C_{\text{Cpx}/\text{熔体}} D_i$  计算获得粒间熔体的某元素含量(图2)。

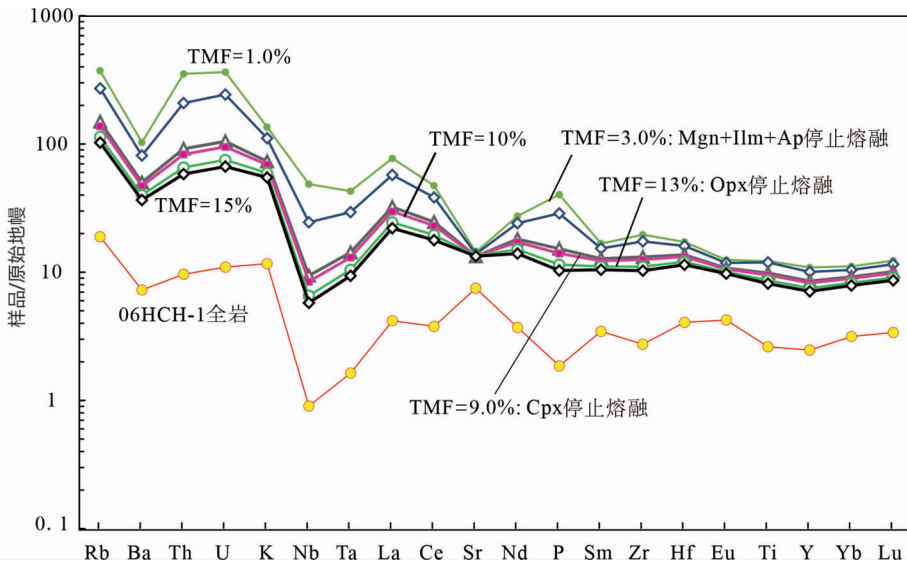


图2 基于单斜辉石平衡配分法和非实比熔融反演获得的母岩浆成分

以晚古生代延边地区清沟山辉长岩样品 06HCH-1 为例计算获得了不同粒间熔体比例(TMf)对应的计算结果(Guo *et al.*, 2016);随着 TMf 的增加,对应的矿物组成和含量变化情况见表 1;当单斜辉石停止熔融后(TMf ≥ 9.0%, TMf 为粒间熔体百分含量),所恢复的母岩浆成分在原始地幔标准化不相容元素蛛网图上呈现出相对一致的配分曲线;通过在副矿物中设置一定的磷灰石含量,可以有效地去除全岩样品在元素 P 的负异常。原始地幔标准化值参考 Sun and McDonough (1989),后图同

Fig. 2 The estimated parent magma composition based on equilibrium distribution method of clinopyroxene and non-modal melting backstripping procedure

A Late Paleozoic gabbro (06HCH-1) at Qinggoushan from Yanbian area in NE China to show the calculation results of different trapped melt fractions (TMF, Guo *et al.*, 2016). Following an increase of TMF, the corresponding variations in mineral assemblage and modal composition are listed in Table 1. When the clinopyroxene is exhausted and the TMF exceeds 9%, the calculated parent magma compositions show consistent primitive mantle trace element spidergrams regardless of TMF. We also set up a little apatite in the modal mineral composition to effectively eliminate the negative P anomaly observed in the whole-rock sample. The trace element values of primitive mantle (PM) refer to Sun and McDonough (1989) and hereafter

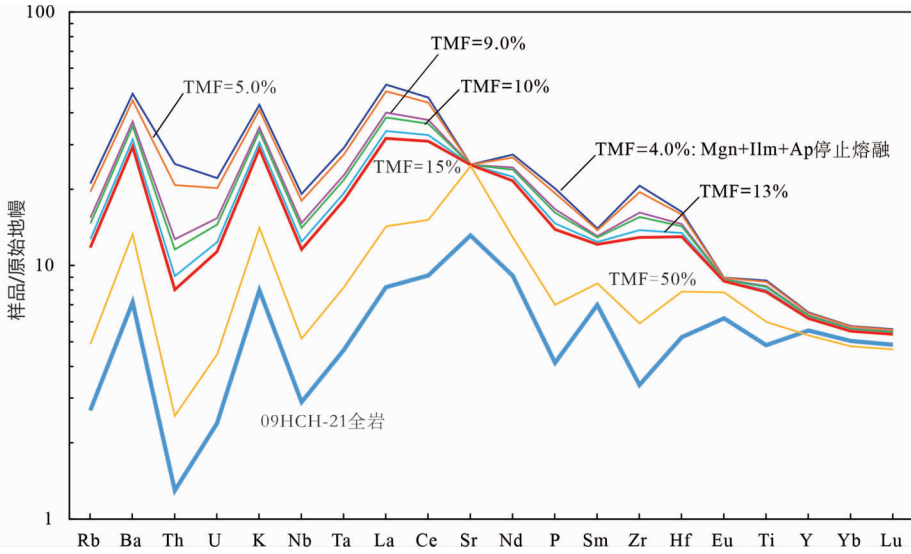


图3 基于角闪石平衡配分法和非实比熔融反演获得的母岩浆成分

以珥春曙光角闪辉长岩样品09HCH-21为例计算获得了不同粒间熔体比例对应的计算结果(Guo *et al.*, 2016). 随着TMF的增加,对应的矿物组成和含量变化情况见表2. 当副矿物停止熔融和TMF $\geq$ 9%后,恢复的母岩浆成分在原始地幔标准化不相容元素蛛网图上呈现出相对一致的配分曲线;当TMF=15%时,所获得的母岩浆没有Sr-Eu异常. 全岩中的Zr异常通过增加微量的锆石(0.01%)予以有效去除. 一旦TMF=50%,全岩测试成分和计算获得的母岩浆成分在不相容元素蛛网图上配分曲线形态基本一致

Fig. 3 The estimated parent magma composition based on equilibrium distribution method of hornblende and non-modal melting backstripping procedure

A Late Paleozoic hornblende gabbro (09HCH-21) at Shuguang from Yanbian area to show the calculation results of different TMF (Guo *et al.*, 2016). Following an increase of TMF, the corresponding variations in mineral assemblage and modal composition are listed in Table 2. When the accessory minerals are exhausted and the TMF exceeds 9%, the calculated parent magma compositions show consistent primitive mantle-normalized trace element spidergrams regardless of TMF. The positive Sr-Eu anomalies disappear when the TMF  $\geq$  15%. The bulk-rock negative Zr anomaly is effectively eliminated by setup of a little zircon in the modal mineral compositions. When the TMF > 50%, the calculated melt composition is quite similar to the bulk rock

类似地,俯冲带的镁铁质岩浆显示出富水特征(Plank *et al.*, 2013),因此出露更多以角闪石为主的超基性-基性侵入岩,我们根据其各类矿物组合、成分和全岩SiO<sub>2</sub>含量可以划分为角闪石岩、角闪辉石岩、角闪辉长岩或辉石闪长岩. 其矿物组合通常为角闪石+/-单斜辉石+斜长石+副矿物,橄榄石和斜方辉石少见. 在计算这类岩石的母岩浆成分时,我们将角闪石当作是未知量,通过计算角闪石中元素的含量来获得平衡粒间熔体的目标元素含量.

$$C_i^{\text{全岩}} = \varphi^{\text{Hb}} C_i^{\text{Hb}} + \varphi^{\text{Cpx}} C_i^{\text{Cpx}} + \varphi^{\text{Pl}} C_i^{\text{Pl}} + \varphi^{\text{副矿物}} C_i^{\text{副矿物}} + \varphi^{\text{TM}} C_i^{\text{TM}} \quad (4)$$

$\varphi$ 代表了各种矿物或粒间熔体的质量百分数. 副矿物主要考虑铁钛氧化物如磁铁矿、钛铁矿、铬铁矿等,其它副矿物有锆石/斜锆石、榍石、磷灰石等.

$$\begin{aligned} C_i^{\text{Hb}} &= C_i^{\text{Pl}} \left( \frac{\text{Hb/熔体}}{\text{Pl/熔体}} D_i \right) = C_i^{\text{Cpx}} \left( \frac{\text{Hb/熔体}}{\text{Cpx/熔体}} D_i \right) \\ &= C_i^{\text{Il}} \left( \frac{\text{Hb/熔体}}{\text{Il/熔体}} D_i \right) = C_i^{\text{Mt}} \left( \frac{\text{Hb/熔体}}{\text{Mt/熔体}} D_i \right) \\ &= C_i^{\text{Ap}} \left( \frac{\text{Hb/熔体}}{\text{Ap/熔体}} D_i \right) = C_i^{\text{Tn}} \left( \frac{\text{Hb/熔体}}{\text{Tn/熔体}} D_i \right) \\ &= C_i^{\text{Zr}} \left( \frac{\text{Hb/熔体}}{\text{Zr/熔体}} D_i \right) \end{aligned} \quad (5)$$

同样地,我们将等式(5)代入到等式(4),此时也只有 $\varphi^{\text{TM}}$ 是一个未知数,只要设定不同的 $\varphi^{\text{TM}}$ ,就可以获得角闪石的某元素含量:

$$\begin{aligned} C_i^{\text{Hb}} &= C_i^{\text{全岩}} / (\varphi^{\text{Hb}} + \varphi^{\text{Cpx}} \times \text{Cpx/熔体} D_i / \text{Hb/熔体} D_i + \\ &\varphi^{\text{Pl}} \times \text{Pl/熔体} D_i / \text{Hb/熔体} D_i + \varphi^{\text{Mt}} \times \text{Mt/熔体} D_i / \text{Hb/熔体} D_i + \\ &\varphi^{\text{Il}} \times \text{Il/熔体} D_i / \text{Hb/熔体} D_i + \varphi^{\text{Ap}} \times \text{Ap/熔体} D_i / \text{Hb/熔体} D_i + \\ &\varphi^{\text{Tn}} \times \text{Tn/熔体} D_i / \text{Hb/熔体} D_i + \varphi^{\text{Zr}} \times \text{Zr/熔体} D_i / \text{Hb/熔体} D_i + \\ &\varphi^{\text{TM}} \times \text{Hb/熔体} D_i) \end{aligned} \quad (6)$$

一旦获得了角闪石中某元素含量,其对应的粒间熔体成分就可以很容易通过等式 $C_i^{\text{熔体}} = C_i^{\text{Hb}} / \text{Hb/熔体} D_i$ 计算出来(图3).

在实际计算过程中,各种矿物的分配系数对于最终结果起到非常重要的作用,因此我们在分配系数的选择上需要非常谨慎. 在玄武岩体系中,不同成分对应的镁铁质造岩矿物和副矿物的分配系数变化非常大,因此我们在选择分配系数时要确保一致性和适用性(Rollinson, 1993). 如在碱性玄武岩和拉斑玄武岩体系中,单斜辉石的REE和Sr分配系数就变化非常大. 此外,由于以前用火山岩中的斑晶/基质含量比值获得的分配系数没有确保二者之间的平衡,因此很多分配系数都存在问题,我们尽可能选择近年来通过实验方法获得的矿物/玄武岩分配系数. 在部分矿物/熔体分配系数无法获得的情况下,比如一些副矿物的分配系数还较为缺乏,也可以根据元素在矿物中的相容性进行合理的假设. 由

表1 非实比熔融下矿物相变的反剥离计算流程 (适用于橄榄辉长岩或苏长岩)

Table 1 The phase change in non-modal melting backstripping procedure (for olivine gabbro or norite)

粒间熔体比例 (%)	熔融方式与比例	矿物相变
0 ~ 3%	Mt + Ilm + Ap 进入熔体	副矿物溶解消失进入熔体
3%	Mt + Ilm + Ap + Ttn 熔融完毕	熔体中的副矿物消失
3% ~ 9%	Cpx/Opx/Pl/Ol 0.429/0.286/0.429/ -0.144	辉石与斜长石熔融, 生成熔体与橄榄石
9%	单斜辉石消失	单斜辉石完全熔融进入熔体
9% ~ 13%	Cpx/Opx/Pl/Ol 0/0.5/0.75/ -0.25	斜方辉石和斜长石发生熔融, 生成熔体与橄榄石
13%	斜方辉石消失	斜方辉石完全熔融进入熔体
13% ~ 90%	Cpx/Opx/Pl/Ol 0/0/0.6/0.4	斜长石与橄榄石发生熔融生成熔体

注: Ol-橄榄石; Opx-斜方辉石; Cpx-单斜辉石; Hb-角闪石; Pl-斜长石; Mt-磁铁矿; Ilm-钛铁矿; Ap-磷灰石; Ttn-榍石; Zr-锆石. 表2同

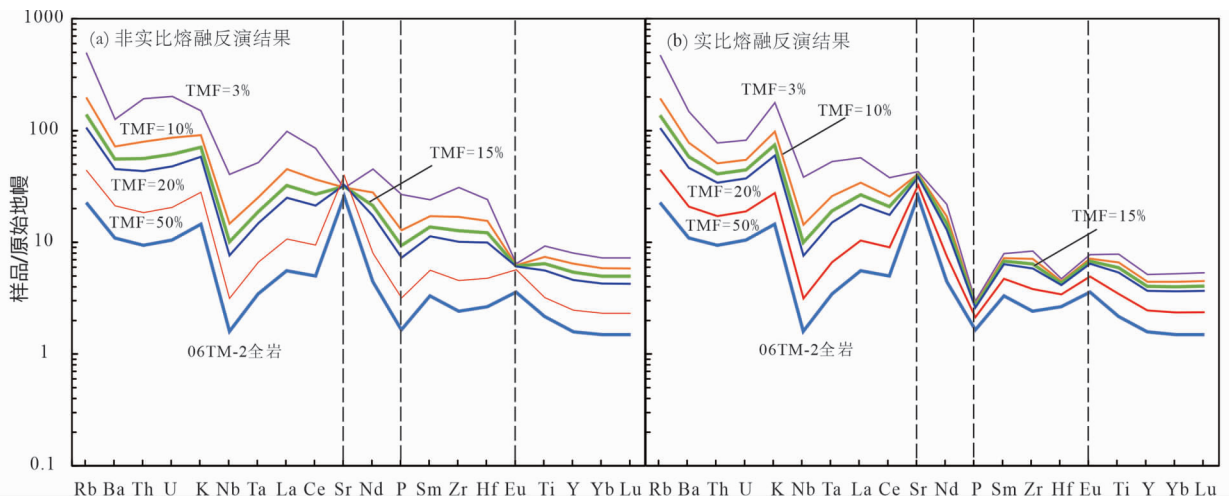


图4 运用非实比与实比熔融反演获得的母岩浆成分对比

(a) 样品 06TM-2 的非实比熔融反演结果, 当 TMF 变化在 10% ~ 15% 时, Sr-Eu 正异常消失, P 的负异常也表现不明显 (Guo *et al.*, 2015);

(b) 06TM-2 的实比熔融反演结果, Sr-Eu 正异常被一致保留, 且 P 负异常明显

Fig. 4 Compositional comparison of parent magmas calculated by non-modal and modal melting back stripping procedures

(a) results of varying TMFs through a non-modal melting back stripping procedure show that the positive Sr-Eu anomalies and negative P anomaly in whole rock Sample 06TM-2 can be effectively eliminated with a TMF range of 10% ~ 15% (Guo *et al.*, 2015); (b) the positive Sr-Eu anomalies and negative P anomaly in whole-rock Sample 06TM-2 remains clear when a modal melting back stripping procedure is applied

于我们的方法主要建立在单斜辉石和角闪石的分配系数基础上, 因此这两种矿物在不同性质熔体中的分配系数选择就显得格外重要, 直接影响最终的计算结果。各种矿物的分配系数可以浏览网站: <https://earthref.org/KDD-old/>。

## 2 非实比熔融的反剥离计算流程

为了获得粒间熔体的成分, 我们采取反剥离方法来开展计算。首先将粒间熔体当作非实比熔融作用 (non-modal melting) 的产物 (Zou *et al.*, 2000), 即部分熔融过程中, 残留

相中各种矿物的比例会不断发生变化 (图 2、图 3)。如副矿物由于其熔点低, 优先进入熔体, 其次是单斜辉石和斜长石, 再次为斜方辉石, 最后是橄榄石发生熔融。不同熔融阶段的具体矿物相变化见表 1 (Bédard, 2001)。我们选择一件辉长岩样品进行了对比计算 (图 4), 发现通过非实比熔融反演的结果更加接近其真实成分。

当我们选择角闪石为未知变量时, 同样也要考虑非实比熔融过程, 其矿物相变过程见表 2。

为了验证方法的正确性, 我们假设一系列不同的 TMF 值。比如说在辉长岩体系的计算中, TMF 越小, 对应粒间熔

表 2 非实比熔融下矿物相变的反剥离流程(适用于角闪辉长岩)

Table 2 The phase change in non-modal melting backstripping procedure (for hornblende gabbro)

粒间熔体比例 (%)	熔融模式	矿物相变
0% ~ 4%	Mt + Ap + Zr + Ttn 进入熔体	副矿物发生熔融
4%	Mt + Ap + Zr + Ttn 熔融完毕	副矿物完全消失
4% ~ 50%	Hb/Pl/Cpx 0.6/0.6/-0.2	角闪石与斜长石熔融生成熔体和单斜辉石

注:副矿物的组成和比例可以根据实际岩相学观察结果进行修改或调整

体的某元素含量越高,一旦 TMF 达到某一变化区间时,获得的微量元素蛛网图的配分模式将一致保持不变,而一旦 TMF > 50%,获得的熔体组分已经非常接近全岩成分,当 TMF = 90%,计算获得的粒间熔体成分与全岩的测试成分几乎一致。

归结起来,镁铁质堆晶岩的计算过程包括以下六个步骤:(1)通过化学方法分析测试获取镁铁质堆晶岩的化学成分,包括主要氧化物和微量元素含量;(2)实际观测或者通过 CIPW 获得各主要造岩矿物和副矿物的质量百分数;(3)选择合适的分配系数,并计算体系的总体分配系数;(4)计算非实比熔融过程中矿物比例的变化;(5)通过公式第二部分中等式(3)和(6)获取单斜辉石和角闪石在不同 TMF 的元素含量;(6)最后获得不同 TMF 的各目标元素含量。

### 3 应用实例

前面已经介绍了平衡配分法的原理和计算过程,接下来介绍一些研究实例来说明平衡配分方法在镁铁质堆晶岩母岩浆恢复中的实效性。

#### 3.1 东北早中生代古太平洋板块俯冲带超镁铁质-镁铁质侵入杂岩

我国东北吉林-黑龙江东部地区呈北东向发育了一系列早侏罗世超镁铁质-镁铁质侵入杂岩,从小兴安岭一直延续到长白山,其岩石类型包括橄榄辉长岩、角闪辉长岩、辉石闪长岩和角闪石岩等(Yu *et al.*, 2012; Guo *et al.*, 2015; Zhang *et al.*, 2016; Yang *et al.*, 2018; ; Ge *et al.*, 2019; Zhao *et al.*, 2019)。部分岩石表现出一定程度的斜长石堆晶结构,在微量元素地球化学特征上为 Sr-Eu 正异常,甚至很多岩石的 REE 配分模式显示出明显的 MREE 富集,显然受到了单斜辉石和/或角闪石的控制(Yu *et al.*, 2012; Guo *et al.*, 2015; Zhang *et al.*, 2016)。对于这些镁铁质-超镁铁质岩石成因的认识也存在分歧,或认为是古太平洋板块俯冲成因,或认为是弧后盆地拉张作用的结果。我们在研究图门超镁铁质-镁铁质侵入杂岩时对典型样品进行了母岩浆恢复(Guo *et al.*, 2015),发现这些不同类型岩石的母岩浆组成非常接近,均属于钙碱性玄武岩/玄武安山岩,并具有典型的弧岩浆

微量元素地球化学特征(图 5),如富集大离子亲石元素和轻稀土元素,亏损高场强元素,为此我们提出古太平洋板块向东亚大陆边缘俯冲的起始时间为早侏罗世,并进一步根据南北两段之间的元素-同位素组成差异,提出了北段的小兴安岭地区为大洋弧,而南段的张广才岭-延边地区为大陆弧(Guo *et al.*, 2015; Zhao *et al.*, 2019)。Zhang *et al.* (2016) 根据我们提供的方法对东北地区如辽宁北部和吉林中部的早-中侏罗世镁铁质堆晶岩进行了类似的母岩浆成分计算,获得了相似的研究结果,认为这些镁铁质堆晶岩是古太平洋板块俯冲作用的产物。

#### 3.2 延边地区晚古生代古亚洲洋俯冲带超镁铁质-镁铁质侵入杂岩

在吉林省东部的延边地区,广泛发育了二叠纪超镁铁质-镁铁质侵入杂岩,岩石类型与早中生代东北地区类似,包括橄榄辉长岩、苏长岩、角闪辉长岩和辉石闪长岩等(李红霞等, 2010; Cao *et al.*, 2013; Zhou *et al.*, 2014; Sun *et al.*, 2015; Guo *et al.*, 2016; 冯光英等, 2018; Yang *et al.*, 2019)。在 REE 配分模式和微量元素蛛网图上,存在多种类型,比如曙光角闪石辉长岩强烈亏损 Th 和 Zr,来自汪清的部分辉长闪长岩样品存在 P 正异常,少量来自前山的辉长岩显示出明显的 Th-U 正异常,这些都是堆晶作用的结果(Guo *et al.*, 2016)。面对如此复杂的岩石组合,只有通过母岩浆成分恢复才可能进行对比。为此,我们分别用单斜辉石和角闪石来开展这些堆晶岩的母岩浆成分。

清沟山辉长岩的计算结果显示其母岩浆为钙碱性玄武岩,除了 Ba 与 Nb-Ta 相对亏损外,总体上具有相对平滑的不相容元素蛛网图(图 6a)。而曙光角闪辉长岩的全岩成分变化起伏非常大,出现明显的 Rb、Th-U、Nb-Ta、P 和 Zr 负异常(图 6b)。运用平衡计算方法获得的母岩浆成分属于拉斑质玄武岩,其亏损 Nb-Ta 和低 Rb 的特征与其极为亏损的 Nd-Hf 同位素组成相对应(Guo *et al.*, 2016),反映其交代介质主要为板片流体。

#### 3.3 东南沿海地区早白垩世超基性-基性侵入杂岩

在东南沿海地区发育了早白垩世超基性-基性侵入杂岩,如在福建省从平潭、泉州到漳州沿北东向分布了多个角

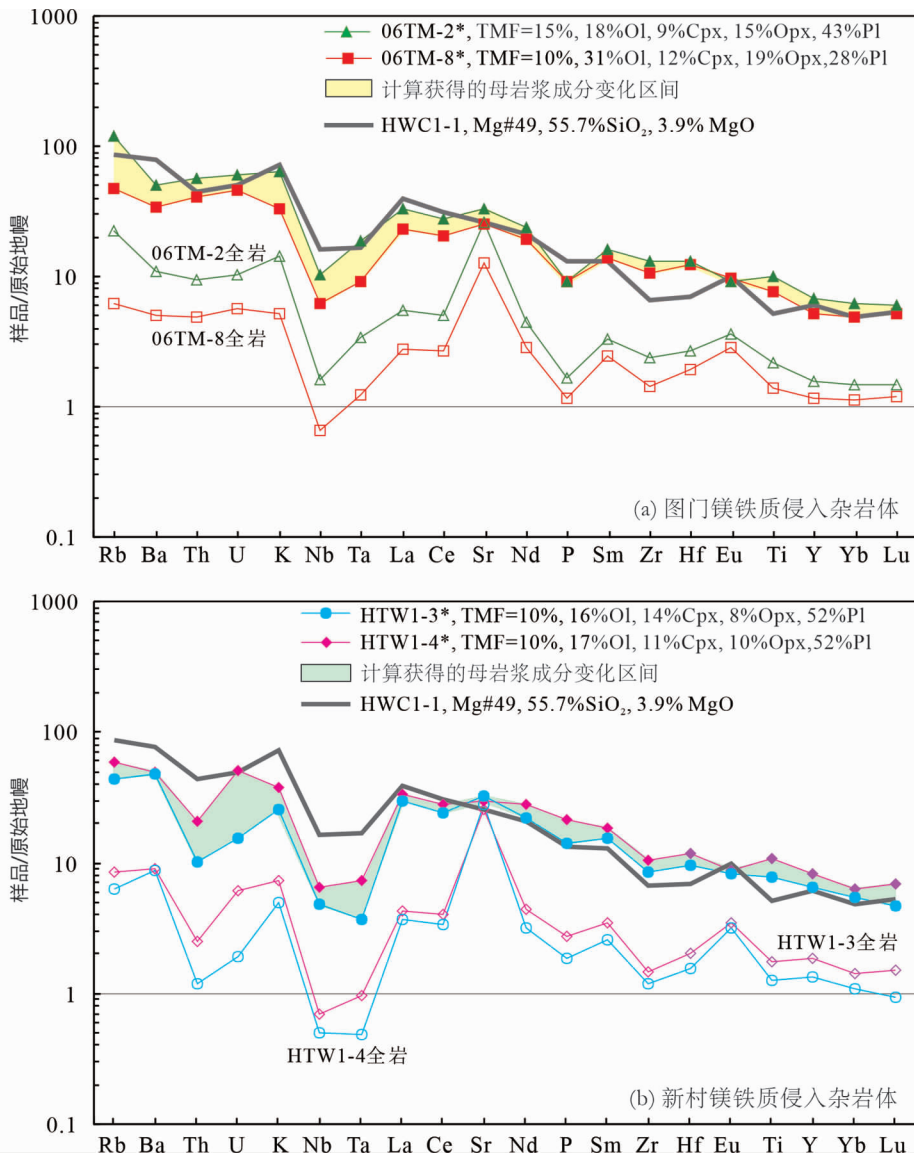


图5 中国东北吉黑地区早侏罗世镁铁质堆晶岩的母岩浆成分计算结果

(a) 延边地区图门超镁铁质-镁铁质侵入杂岩体, 06TM-2 和-8 均为橄榄辉长岩 (Guo *et al.*, 2015); (b) 小兴安岭新村辉长岩侵入体, 全岩原始数据来自 Yu *et al.* (2012); 样品号后面带星号为计算结果, 后同

Fig. 5 Calculated parental magma compositions of the Jurassic mafic cumulates in Jilin-Heilongjiang area of NE China

(a) olivine gabbros (06TM-2 and -8) from the Tumen mafic intrusive complex (Guo *et al.*, 2015); (b) gabbros from the Xincun mafic intrusion (Yu *et al.*, 2012). The sample names with stars denote the estimated parent magma compositions in equilibrium with the mineral assemblage and hereafter

闪石辉长岩体 (董传万等, 1997; Xu *et al.*, 1999; Zhou and Li, 2000; Li *et al.*, 2012; Chen *et al.*, 2013; Zhang *et al.*, 2019; Guo *et al.*, 2021), 这些岩石不仅具有明显的 Sr-Eu 正异常, 同时由于角闪石堆晶作用或者是榍石/钛铁矿的存在, 不同程度地显示出 Ti 正异常。尽管前人对这些侵入岩开展了大量的研究, 认为其岩石成因与古太平洋俯冲作用相关, 但是关于其形成环境和岩浆演化也存在争议。比如这些侵入岩都显示出相对富集的同位素组成, 被认为可能与地壳混染或 AFC 过程有关; 另外, 根据传统的地球化学判别方法, 这些富 Ti 的基性岩可能形成于弧后伸展环境。为此我们开

展了母岩浆的恢复计算, 其结果显示, 平潭、岱前山和泉州三个岩体的母岩浆成分具有完全一致的微量元素蛛网图样式 (图7), 亏损 HFSE 和富集 LILE 与 LREE, 与典型的俯冲带钙碱性玄武岩相似 (Zhang *et al.*, 2019)。富 Ti 特征主要是由于存在较多的榍石与钛铁矿所致。我们的研究结果确定了东南沿海早白垩世超基性-基性侵入杂岩与古太平洋板块俯冲之间的内在联系, 大量的俯冲沉积物熔体改造的地幔楔熔融形成了这些具有 Sr-Nd-Pb-Hf 同位素富集的镁铁质岩浆, 并提出当时为相对较热的俯冲带, 类似于新生代的日本西南和现代小安德烈斯俯冲带 (Shimoda *et al.*, 1998; Carpentier

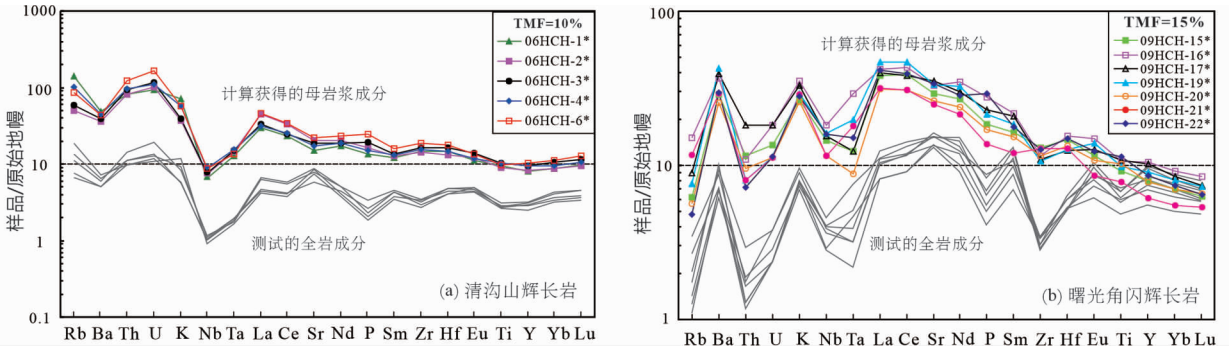


图6 延边地区晚古生代镁铁质侵入岩的母岩浆成分计算结果(据 Guo *et al.*, 2016)

Fig. 6 Calculated parental magma compositions of the Late Paleozoic mafic intrusions in NE China (after Guo *et al.*, 2016)

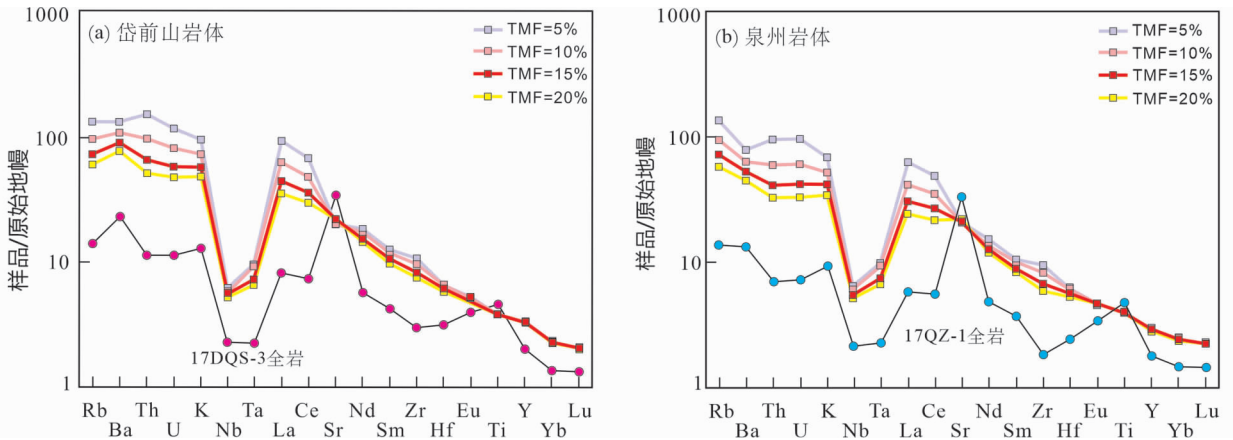


图7 东南沿海地区早白垩世镁铁质侵入岩的母岩浆成分计算结果(据 Zhang *et al.*, 2019)

Fig. 7 Calculated parental magma compositions of the Early Cretaceous hornblende gabbros in the coastal region of SE China (after Zhang *et al.*, 2019)

*et al.*, 2009; Labanieh *et al.*, 2010)。

### 3.4 华南云开地区古生代镁铁质堆晶岩

华南云开地区古生代是否受到来自古特提斯洋的俯冲作用,目前仍存在认识上的分歧(Wang *et al.*, 2007, 2013; Qin *et al.*, 2012; Metcalfe, 2013; Xu *et al.*, 2018; Shu *et al.*, 2021)。我们初步开展了区域古生代镁铁质侵入岩的研究,发现存在多种岩石类型,包括富铁侵入杂岩体、富镁橄榄辉长岩、富钙铝辉长岩和辉绿岩等,同时还有一些中酸性的富碱侵入岩和花岗岩等。尤其是富镁和钙铝的辉长岩都包含斜长石,初步结果显示其 An 牌号甚至大于 95,反映斜长石为早期富水岩浆的结晶产物(Panjasawatwong *et al.*, 1995),与中国东北地区早侏罗世橄榄辉长岩和东南沿海地区早白垩世角闪辉长岩相似(Guo *et al.*, 2015; Zhang *et al.*, 2019),而与典型的陆内环境形成的辉长岩(如济南橄榄辉长岩)主要出现拉长石存在明显差异(Guo *et al.*, 2013)。

与此同时,我们针对具有明显斜长石堆晶结构的富钙铝和富镁辉长岩分别进行了母岩浆成分恢复(图 8),结果显示

这些镁铁质侵入岩具有岛弧型微量元素地球化学特征,结合其富钙斜长石指示初始岩浆富水特点,我们认为它们形成于古特提斯洋的俯冲带环境。

我们将平衡配分法计算获得的母岩浆成分与实测的镁铁质堆晶岩全岩成分进行对比(Guo *et al.*, 2016),重点考察常用于示踪俯冲带地幔楔改造作用的微量元素比值,比如 Ba/REE 和 Ba/HFSE 可以较好地示踪地幔楔是否受到了流体改造,而 Th/REE 则是地幔楔中是否存在俯冲沉积物贡献的地球化学指标(Woodhead *et al.*, 2001)。对比结果显示(图 9),计算获得的母岩浆 Th/La 比值与全岩实测结果吻合最好(图 9a),而 Th/Yb 计算比值则明显偏高(图 9b),计算的 Ba/La 与 Ba/Nb 比值与实测结果相似(图 9c, d)。因此镁铁质堆晶岩全岩的 Th/La、Ba/REE 和 Ba/HFSE 比值适合于开展俯冲带的深部动力学过程研究。

### 3.5 其它研究实例

根据我们提供的计算方法,Dong *et al.* (2018)开展了内蒙古柯丹山阿拉斯加型超镁铁质-镁铁质堆晶岩的母岩浆恢



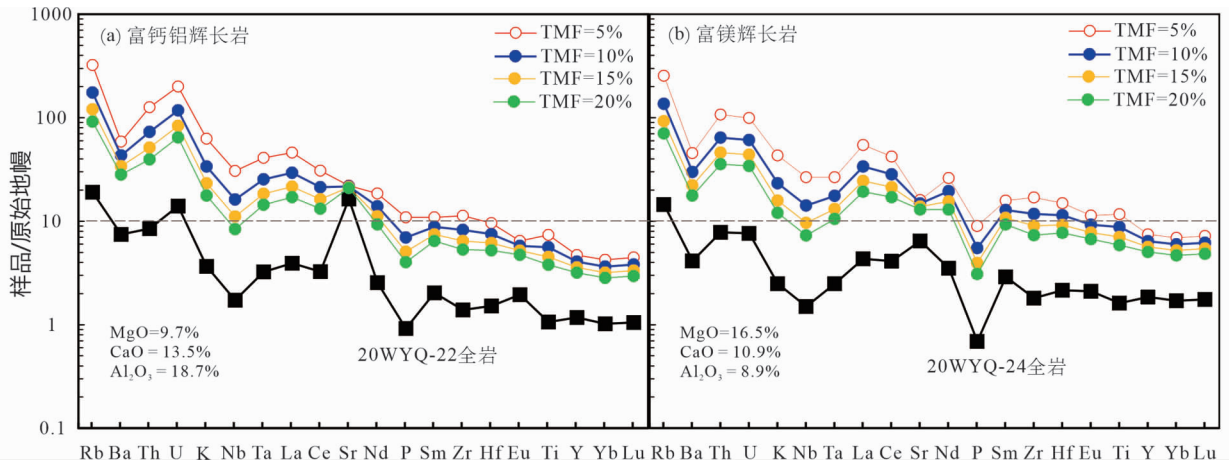


图8 华南云开地区古生代镁铁质侵入岩的母岩浆恢复结果

(a) 富钙铝辉长岩; (b) 富镁辉长岩. 计算结果显示两类镁铁质侵入岩的母岩浆都具有典型岛弧型玄武岩的微量元素地球化学特征

Fig. 8 Calculated parent magma compositions of Paleozoic mafic intrusions in the Yunkai Massif

(a) the Al-rich gabbro; (b) the Ca-rich gabbro. The recalculation results demonstrate that the parent magmas of both mafic rock types have typical arc-type trace element features

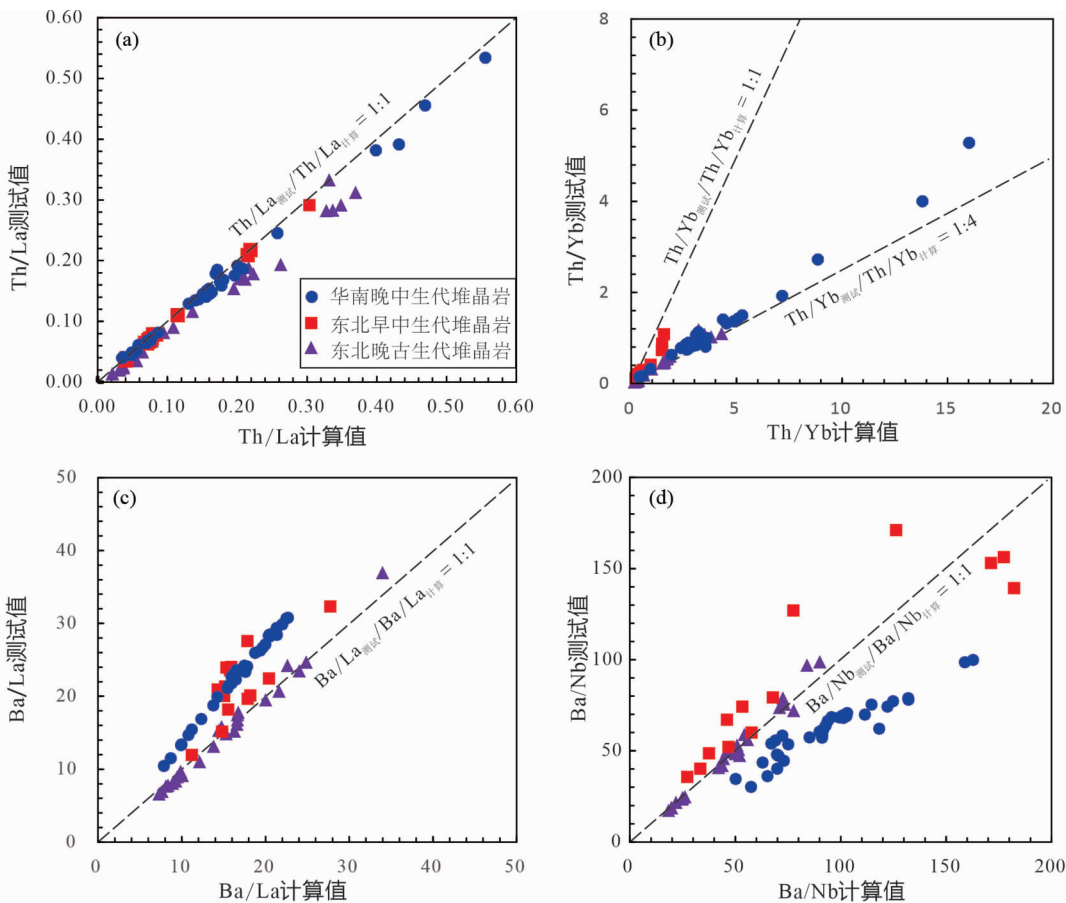


图9 中国东部古生代-中生代镁铁质堆晶岩的微量元素比值的实测与反演计算结果对比

Fig. 9 Comparison of measured and calculated trace elemental ratios of Paleozoic-Mesozoic mafic intrusions in eastern China

复, 认为该岩体的母岩浆具有典型的弧岩浆成分特点。Wang *et al.* (2018) 和 Wang and Wang (2020) 对扬子陆块北缘随

州-枣阳地区震旦纪辉长岩和橄长岩进行了母岩浆成分计算, 其结果指示这些超镁铁质堆晶岩的母岩浆具有相对富集

LREE 和弱亏损 HFSE 的地球化学特征, 结合其负  $\epsilon_{Nd}(t)$  和高放射成因 Os 的同位素组成特点, 认为其来源于交代岩石圈地幔。

Wang *et al.* (2019) 对华南雪峰山隘口和新余地区晚元古代板内镁铁质堆晶岩 (辉石岩) 开展了母岩浆恢复, 其结果指示这些超镁铁质堆晶岩的母岩浆具有类似洋岛玄武岩的微量元素地球化学特征, 反映其形成于板内伸展背景, 为新元古代罗迪尼亚超大陆裂解过程的产物。

平衡配分方法也可以用于月球斜长岩与镁质岩套、蛇绿岩套中超镁铁质-镁铁质堆晶岩、下部洋壳辉长岩和辉石岩等的母岩浆成分恢复。

## 4 结语

超镁铁-镁铁质火成岩的母岩浆恢复方法众多, 比如橄榄石熔体包裹体方法、矿物-熔体平衡配分法等等。但是这些方法主要用于喷出岩, 如橄榄石中熔体包裹体成分可以有效记录橄榄石晶体生长过程中平衡的岩浆成分 (Ren *et al.*, 2005); 矿物的成分环带可以记录岩浆分异、地壳混染和岩浆混合作用等演化过程 (Guo *et al.*, 2007)。通过 LA-ICP-MS 直接分析单斜辉石和角闪石斑晶的微量元素含量, 然后运用矿物/熔体分配系数来计算与单斜辉石或角闪石平衡的熔体成分。然而, 超镁铁-镁铁质侵入岩在地壳岩浆房经历了相对缓慢的冷却、熔离和堆晶作用, 以及岩浆固结后因物理化学条件改变而发生的成分出溶与扩散过程等等, 致使其母岩浆成分的恢复变得非常困难。在这些侵入岩中, 单矿物内部和不同颗粒之间的微量元素含量存在显著变化, 因此选择单矿物的哪类数据 (平均含量、中位数还是其它数据比如高 Mg<sup>#</sup> 部分) 来进行计算带来了诸多不确定性。此外, 目前开展矿物/熔体分配系数研究的岩浆体系比实际观察到的超镁铁质-镁铁质侵入岩的组成要简单得多, 如何确定单斜辉石/角闪石在镁铁质岩浆逐渐冷却过程的分配系数变化也非常困难。本文的计算方法是基于岩相学观察到的矿物组合进行加权平均, 获得的结果对应了与堆晶矿物组合平衡的母岩浆成分, 相对于单矿物-熔体平衡分配的计算结果应该更加令人信服。

尽管我们建立的镁铁质堆晶岩母岩浆恢复方法为应用他们的地球化学特征来示踪古俯冲带/造山带演化提供了可能, 但是在实际运用中仍然存在一定的不确定性: (1) 部分镁铁质堆晶岩具有异常低的 Th-U 和 Zr-Hf 含量, 有可能因为样品分析过程中锆石/斜锆石没有完全溶解造成的, 因此这类样品不适合开展其母岩浆成分的恢复计算。在开展母岩浆成分计算中首先要对分析数据质量进行甄别。(2) 镁铁质-超镁铁质堆晶岩的母岩浆成分恢复主要基于矿物与粒间熔体之间的平衡关系, 如果岩石固结后明显受到了后期流体/熔体的改造, 或者在岩浆上升过程中存在明显的地壳混染或 AFC 过程影响。这类样品也不适合开展母岩浆的成分恢复。

(3) 在母岩浆成分计算过程中可以通过增减副矿物如磷灰石、铁钛氧化物、榍石、锆石/斜锆石来解决一些镁铁质堆晶岩中除了显示出明显的 Sr-Eu 正异常外, 还存在 P、Ti、Th-U 和 Zr-Hf 等元素的异常。具体增减的副矿物种类与成分应该遵循岩相学的观察结果。(4) 在古老俯冲带重建和恢复中, 尽可能采用玄武岩或者基性岩脉如辉绿岩和熔体包裹体的化学和同位素组成来示踪岩浆演化和地幔楔富集改造过程。在上述岩石类型缺乏的情况下, 开展镁铁质堆晶岩的母岩浆计算方法也可以获得相应不错的结果。(5) 对比镁铁质堆晶岩的全岩实测成分和计算的母岩浆微量元素组成, 我们认为利用这类岩石的 Th/La、Ba/REE 和 Ba/HFSE 比值可以用来示踪地幔楔的改造作用, 而实测的 Th/Yb 比值相较计算值显著偏低, 该比值不适用讨论俯冲带中沉积物的贡献。

谨以此文庆祝周新华老师八十年华诞。我与周老师相识多年, 他为人师表, 待人和蔼, 亦师亦友, 不断鼓励我们年轻人积极投身祖国的地质科研中。我曾经陪同周老师到我国东北地区和蒙古国中东部地区开展了多次野外考察, 得到了周老师很多学术上的帮助和人生教诲, 让我受益匪浅, 终身难忘。

**致谢** 本文的最终成文受益于两位审稿专家的意见, 在此深表感谢!

## References

- Bédard JH. 1994. A procedure for calculating the equilibrium distribution of trace elements among the minerals of cumulate rocks, and the concentration of trace elements in the coexisting liquids. *Chemical Geology*, 118(1-4): 143-153
- Bédard JH. 2001. Parental magmas of the Nain Plutonic Suite anorthosites and mafic cumulates: A trace element modelling approach. *Contributions to Mineralogy and Petrology*, 141(6): 747-771
- Bédard JH, Leclerc F, Harris LB and Goulet N. 2009. Intra-sill magmatic evolution in the Cummings Complex, Abitibi greenstone belt: Tholeiitic to calc-alkaline magmatism recorded in an Archean subvolcanic conduit system. *Lithos*, 111(1-2): 47-71
- Cao HH, Xu WL, Pei FP, Wang ZW, Wang F and Wang ZJ. 2013. Zircon U-Pb geochronology and petrogenesis of the Late Paleozoic-Early Mesozoic intrusive rocks in the eastern segment of the northern margin of the North China Block. *Lithos*, 170-171: 191-207
- Carpentier M, Chauvel C, Maury RC and Mattielli N. 2009. The "zircon effect" as recorded by the chemical and Hf isotopic compositions of Lesser Antilles forearc sediments. *Earth and Planetary Science Letters*, 287(1-2): 86-99
- Chen JY, Yang JH, Zhang JH, Sun JF and Wilde SA. 2013. Petrogenesis of the Cretaceous Zhangzhou batholith in southeastern China: Zircon U-Pb age and Sr-Nd-Hf-O isotopic evidence. *Lithos*, 162-163: 140-156
- Davies JH and Stevenson DJ. 1992. Physical model of source region of subduction zone volcanics. *Journal of Geophysical Research: Solid Earth*, 97(B2): 2037-2070
- Dong CW, Zhou XM, Li HM, Ren SL and Zhou XH. 1997. Late Mesozoic crust-mantle interaction in southeastern Fujian: Isotopic evidence from the Pingtan igneous complex. *Chinese Science Bulletin*, 42(6): 495-498

- Dong JL, Song SG, Wang MM, Allen MB, Su L, Wang C, Yang LM and Xu B. 2018. Alaskan-type Kedanshan intrusion (central Inner Mongolia, China): Superimposed subduction between the Mongol-Okhotsk and Paleo-Pacific oceans in the Jurassic. *Journal of Asian Earth Sciences*, 167: 68–81
- Feng GY, Liu S, Niu XL and Yang JS. 2018. Geochronology, geochemistry and petrogenesis of Early-Middle Permian mafic intrusion in Zhangguangcai Range, China. *Earth Science (Journal of China University of Geosciences)*, 43(4): 1293–1306 (in Chinese with English abstract)
- Ge MH, Zhang JJ, Li L and Liu K. 2019. Ages and geochemistry of Early Jurassic granitoids in the Lesser Xing'an-Zhangguangcai Ranges, NE China: Petrogenesis and tectonic implications. *Lithosphere*, 11(6): 804–820
- Grove TL, Chatterjee N, Parman SW and Médard E. 2006. The influence of H<sub>2</sub>O on mantle wedge melting. *Earth and Planetary Science Letters*, 249(1–2): 74–89
- Guo F, Nakamura E, Fan WM, Kobayoshi K and Li CW. 2007. Generation of Palaeocene adakitic andesites by magma mixing, Yanji area, NE China. *Journal of Petrology*, 48(4): 661–692
- Guo F, Guo JT, Wang CY, Fan WM, Li CW, Zhao L, Li HX and Li JY. 2013. Formation of mafic magmas through lower crustal AFC processes: An example from the Jinan gabbroic intrusion in the North China Block. *Lithos*, 179: 157–174
- Guo F, Li HX, Fan WM, Li JY, Zhao L, Huang MW and Xu WL. 2015. Early Jurassic subduction of the Paleo-Pacific Ocean in NE China: Petrologic and geochemical evidence from the Tumen mafic intrusive complex. *Lithos*, 224–225: 46–60
- Guo F, Li HX, Fan WM, Li JY, Zhao L and Huang MW. 2016. Variable sediment flux in generation of Permian subduction-related mafic intrusions from the Yanbian region, NE China. *Lithos*, 261: 195–215
- Guo F, Wu YM, Zhang B, Zhang XB, Zhao L and Liao J. 2021. Magmatic responses to Cretaceous subduction and tearing of the paleo-Pacific Plate in SE China: An overview. *Earth-Science Reviews*, 212: 103448
- Labanih S, Chauvel C, Germa A, Quidelleur X and Lewin E. 2010. Isotopic hyperbolas constrain sources and processes under the Lesser Antilles arc. *Earth and Planetary Science Letters*, 298(1–2): 35–46
- Li HX, Guo F, Li CW and Zhao L. 2010. Late Paleozoic subduction of the Paleo-Asian Ocean: Geochronological and geochemical records from Qianshan mafic intrusion in Hunchun area, NE China. *Acta Petrologica Sinica*, 26(5): 1530–1540 (in Chinese with English abstract)
- Li Z, Qiu JS and Xu XS. 2012. Geochronological, geochemical and Sr-Nd-Hf isotopic constraints on petrogenesis of Late Mesozoic gabbro-granite complexes on the southeast coast of Fujian, South China: Insights into a depleted mantle source region and crust-mantle interactions. *Geological Magazine*, 149(3): 459–482
- Macdonald R, Hawkesworth CJ and Heath E. 2000. The Lesser Antilles volcanic chain: A study in arc magmatism. *Earth-Science Reviews*, 49(1–4): 1–76
- McCulloch MT and Gamble JA. 1991. Geochemical and geodynamical constraints on subduction zone magmatism. *Earth and Planetary Science Letters*, 102(3–4): 358–374
- Metcalfe I. 2013. Gondwana dispersion and Asian accretion: Tectonic and palaeogeographic evolution of eastern Tethys. *Journal of Asian Earth Sciences*, 66: 1–33
- Nichols GT, Wyllie PJ and Stern CR. 1994. Subduction zone melting of pelagic sediments constrained by melting experiments. *Nature*, 371(6500): 785–788
- Panjasawatwong Y, Danyushevsky LV, Crawford AJ and Harris KL. 1995. An experimental study of the effects of melt composition on plagioclase-melt equilibria at 5 and 10kbar: Implications for the origin of magmatic high-An plagioclase. *Contributions to Mineralogy and Petrology*, 118(4): 420–432
- Plank T and Langmuir CH. 1998. The chemical composition of subducting sediment and its consequences for the crust and mantle. *Chemical Geology*, 145(3–4): 325–394
- Plank T, Kelley KA, Zimmer MM, Hauri EH and Wallace PJ. 2013. Why do mafic arc magmas contain ~4wt% water on average? *Earth and Planetary Science Letters*, 364: 168–179
- Qin XF, Wang ZQ, Zhang YL, Pan LZ, Hu GQ and Zhou FS. 2012. Geochemistry of Permian mafic igneous rocks from the Napo-Qinzhou tectonic belt in southwest Guangxi, Southwest China: Implications for arc-back arc basin magmatic evolution. *Acta Geologica Sinica*, 86(5): 1182–1199
- Ren ZY, Ingle S, Takahashi E, Hirano N and Hirata T. 2005. The chemical structure of the Hawaiian mantle plume. *Nature*, 436(7052): 837–840
- Ridolfi F and Renzulli A. 2012. Calcic amphiboles in calc-alkaline and alkaline magmas: Thermobarometric and chemometric empirical equations valid up to 1, 130°C and 2. GPa. *Contributions to Mineralogy and Petrology*, 163(5): 877–895
- Rollinson HR. 1993. *Using Geochemical Data: Evaluation, Presentation, Interpretation*. London: Routledge, 1–352
- Shaw AM, Hauri EH, Fischer TP, Hilton DR and Kelley KA. 2008. Hydrogen isotopes in Mariana arc melt inclusions: Implications for subduction dehydration and the deep-Earth water cycle. *Earth and Planetary Science Letters*, 275(1–2): 138–145
- Shimoda G, Tatsumi Y, Nohda S, Ishizaka K and Jahn BM. 1998. Setouchi high-Mg andesites revisited: Geochemical evidence for melting of subducting sediments. *Earth and Planetary Science Letters*, 160(3–4): 479–492
- Shu LS, Yao JL, Wang B, Faure M, Charvet J and Chen Y. 2021. Neoproterozoic plate tectonic process and Phanerozoic geodynamic evolution of the South China Block. *Earth-Science Reviews*, 216: 103596
- Stern RJ. 2002. Subduction zones. *Reviews of Geophysics*, 40(4): 1012
- Stolz AJ, Jochum KP, Spettel B and Hofmann AW. 1996. Fluid- and melt-related enrichment in the subarc mantle: Evidence from Nb-Ta variations in island-arc basalts. *Geology*, 24(7): 587–590
- Sun MD, Xu YG, Wilde SA, Chen HL and Yang SF. 2015. The Permian Dongfanghong island-arc gabbro of the Wandashan Orogen, NE China: Implications for Paleo-Pacific subduction. *Tectonophysics*, 659: 122–136
- Sun SS and McDonough WF. 1989. Chemical and isotopic systematics of oceanic basalts: Implications for mantle composition and processes. In: Saunders AD and Norry MJ (eds.). *Magmatism in the Ocean Basins*. Geological Society, London, Special Publications, 42(1): 313–345
- Tatsumi Y and Eggins S. 1995. *Subduction Zone Magmatism*. Cambridge: Blackwell Science Publication, 1–211
- Tollstrup DL and Gill JB. 2005. Hafnium systematics of the Mariana arc: Evidence for sediment melt and residual phases. *Geology*, 33(9): 737–740
- von Huene R and Scholl DW. 1991. Observations at convergent margins concerning sediment subduction, subduction erosion, and the growth of continental crust. *Reviews of Geophysics*, 29(3): 279–316
- Wang MX, Wang CY and Wei B. 2018. Platinum-group elemental and Sr-Nd-Os isotopic geochemistry of the ~635Ma mafic intrusions in the northern margin of the Yangtze Block: A link of metasomatized subcontinental lithospheric mantle and Ni-Cu-(PGE) sulfide mineralization. *Precambrian Research*, 309: 325–342
- Wang MX and Wang CY. 2020. Crystal size distributions and trace element compositions of the fluorapatite from the Bijigou Fe-Ti oxide-bearing layered interstitial, central China: Insights for the expulsion processes of interstitial liquid from crystal mush. *Journal of Petrology*, 61(7): ega069
- Wang YJ, Fan WM, Zhang GW and Zhang YH. 2013. Phanerozoic tectonics of the South China Block: Key observations and controversies. *Gondwana Research*, 23(4): 1273–1305
- Wang YJ, Fan WM, Zhao GC, Ji SC and Peng TP. 2007. Zircon U-Pb geochronology of gneissic rocks in the Yunkai massif and its

- implications on the Caledonian event in the South China Block. *Gondwana Research*, 12(4): 404–416
- Wang YJ, Zhang YZ, Cawood PA, Zhou YZ, Zhang FF, Yang X and Cui X. 2019. Early Neoproterozoic assembly and subsequent rifting in South China: Revealed from mafic and ultramafic rocks, central Jiangnan Orogen. *Precambrian Research*, 331: 105367
- Woodhead JD, Hergt JM, Davidson JP and Eggins SM. 2001. Hafnium isotope evidence for ‘conservative’ element mobility during subduction zone processes. *Earth and Planetary Science Letters*, 192(3): 331–346
- Xu WC, Luo BJ, Xu YJ, Wang L and Chen Q. 2018. Geochronology, geochemistry, and petrogenesis of Late Permian to Early Triassic mafic rocks from Darongshan, South China: Implications for ultrahigh-temperature metamorphism and S-type granite generation. *Lithos*, 308–309: 168–180
- Xu XS, Dong CW, Li WX and Zhou XM. 1999. Late Mesozoic intrusive complexes in the coastal area of Fujian, SE China: The significance of the gabbro-diorite-granite association. *Lithos*, 46(2): 299–315
- Yang DG, Sun DY, Hou XG, Mao AQ, Tang ZY and Qin Z. 2018. Geochemistry and zircon Hf isotopes of the Early Mesozoic intrusive rocks in the South Hunchun, Yanbian area, Northeast China: Petrogenesis and implications for crustal growth. *International Geology Review*, 60(8): 1038–1060
- Yang H, Ge WC, Dong Y, Bi JH, Ji Z, He Y, Jing Y and Xu WL. 2019. Permian subduction of the Paleo-Pacific (Panthalassic) oceanic lithosphere beneath the Jiamusi Block: Geochronological and geochemical evidence from the Luobei mafic intrusions in Northeast China. *Lithos*, 332–333: 207–225
- Yu JJ, Wang F, Xu WL, Gao FH and Pei FP. 2012. Early Jurassic mafic magmatism in the Lesser Xing’an-Zhangguangcai Range, NE China, and its tectonic implications: Constraints from zircon U-Pb chronology and geochemistry. *Lithos*, 142–143: 256–266
- Zack T and John T. 2007. An evaluation of reactive fluid flow and trace element mobility in subducting slabs. *Chemical Geology*, 239(3–4): 199–216
- Zhang B, Guo F, Zhang XB, Wu YM, Wang GQ and Zhao L. 2019. Early Cretaceous subduction of Paleo-Pacific Ocean in the coastal region of SE China: Petrological and geochemical constraints from the mafic intrusions. *Lithos*, 334–335: 8–24
- Zhang HH, Wang F, Xu WL, Cao HH and Pei FP. 2016. Petrogenesis of Early-Middle Jurassic intrusive rocks in northern Liaoning and central Jilin provinces, northeast China: Implications for the extent of spatial-temporal overprinting of the Mongol-Okhotsk and Paleo-Pacific tectonic regimes. *Lithos*, 256–257: 132–147
- Zhao L, Guo F, Fan WM and Huang MW. 2019. Roles of subducted pelagic and terrigenous sediments in Early Jurassic mafic magmatism in NE China: Constraints on the architecture of paleo-Pacific subduction zone. *Journal of Geophysical Research: Solid Earth*, 124(3): 2525–2550
- Zhou JB, Cao JL, Wilde SA, Zhao GC, Zhang JJ and Wang B. 2014. Paleo-Pacific subduction-accretion: Evidence from Geochemical and U-Pb zircon dating of the Nadanhada accretionary complex, NE China. *Tectonics*, 33(12): 2444–2466
- Zhou XM and Li WX. 2000. Origin of Late Mesozoic igneous rocks in southeastern China: Implications for lithosphere subduction and underplating of mafic magmas. *Tectonophysics*, 326(3–4): 269–287
- Zou HB. 2000. Modeling of trace element fractionation during non-modal dynamic melting with linear variations in mineral/melt distribution coefficients. *Geochimica et Cosmochimica Acta*, 64(6): 1095–1102

#### 附中文参考文献

- 董传万, 周新民, 李惠民, 任胜利, 周新华. 1997. 闽东南晚中生代的壳幔作用: 平潭火成杂岩的同位素证据. *科学通报*, 42(9): 959–962
- 冯光英, 刘燊, 牛晓露, 杨经绥. 2018. 张广才岭地块早-中二叠世镁铁质侵入岩体的年代学、地球化学及岩石成因. *地球科学(中国地质大学学报)*, 43(4): 1293–1306
- 李红霞, 郭锋, 李超文, 赵亮. 2010. 晚古生代古亚洲洋俯冲作用: 来自珙春前山镁铁质侵入岩的年代学和地球化学记录. *岩石学报*, 26(5): 1530–1540